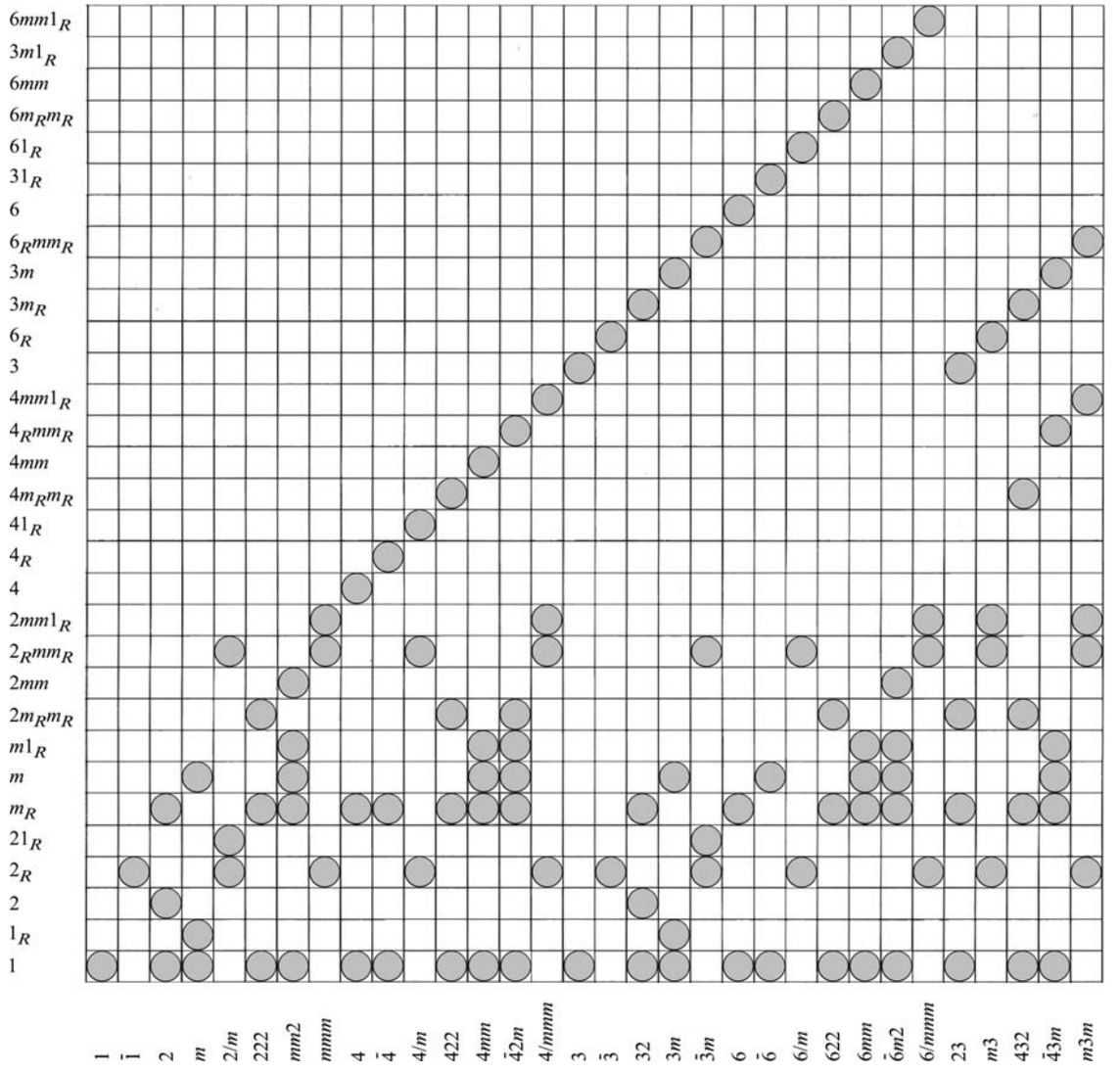

Fig. 2.5.3.4. Relation between diffraction groups and crystal point groups (after Buxton *et al.*, 1976).

lines are seen in the ZOLZ discs, the symmetry elements found from the CBED patterns are only those of the specimen projected along the zone axis. The projection of the specimen along the zone axis causes horizontal mirror symmetry m', the corresponding CBED symmetry being 1_R. When symmetry 1_R is added to the 31 diffraction groups, ten projection diffraction groups having symmetry symbol 1_R are derived as shown in column VI of Table 2.5.3.3. If only ZOLZ reflections are observed in CBED patterns, a projection diffraction group instead of a diffraction group is obtained, where only the pattern symmetries given in the rows of the diffraction groups having symmetry symbol 1_R in Table 2.5.3.3 should be consulted. Two projection diffraction groups obtained from two different zone axes are the minimum needed to determine a crystal point group, because it is constructed by the three-dimensional combination of symmetry elements. It should be noted that if a diffraction group is determined carelessly from CBED patterns with no HOLZ lines, the wrong crystal point group is obtained.

2.5.3.2.7. Symmetrical many-beam method

In the sections above, the point-group determination method established by Buxton *et al.* (1976) was described, where two- and three-dimensional symmetry elements were determined, respectively, from ZAPs and DPs.

The Laue circle is defined as the intersection of the Ewald sphere with the ZOLZ, and all reflections on this circle are simultaneously at the Bragg condition. If many such DPs are recorded (all simultaneously at the Bragg condition), many three-dimensional symmetry elements can be identified from one photograph. Using a group-theoretical method, Tinnappel (1975) studied the symmetries appearing in simultaneously excited DPs for various combinations of crystal symmetry elements. Based upon his treatment, Tanaka, Saito & Sekii (1983) developed a method for determining diffraction groups using simultaneously excited symmetrical hexagonal six-beam, square four-beam and rectangular four-beam CBED patterns. All the CBED symmetries appearing in the symmetrical many-beam (SMB) patterns were derived by the graphical method used in the paper of Buxton *et al.* (1976). From an experimental viewpoint, it is advantageous that symmetry elements can be identified from one photograph. It was found that twenty diffraction groups can be identified from one SMB pattern, whereas ten diffraction groups can be determined by Buxton *et al.*'s method. An experimental comparison between the two methods was performed by Howe *et al.* (1986).

SMB patterns are easily obtained by tilting a specimen crystal or the incident beam from a zone axis into an orientation to excite low-order reflections simultaneously. Fig. 2.5.3.7 illustrates the symmetries of the SMB patterns for all the diffraction groups except for the five groups 1, 1_R, 2, 2_R and 21_R. For these groups, the two-beam method for exciting one reflection is satisfactory because many-beam excitation gives no more information than the two-beam case. In the six-beam and square four-beam cases,

Table 2.5.3.4. *Diffraction groups expected at various crystal orientations for 32 point groups*

This table is adapted from Buxton *et al.* (1976).

	Zone-axis symmetries					
Point group	⟨111⟩	⟨100⟩	⟨110⟩	⟨*uv*0⟩	⟨*uuw*⟩	[*uvw*]
$m3m$	$6_R mm_R$	$4mm1_R$	$2mm1_R$	$2_R mm_R$	$2_R mm_R$	2_R
$\bar{4}3m$	$3m$	$4_R mm_R$	$m1_R$	m_R	m	1
432	$3m_R$	$4m_R m_R$	$2m_R m_R$	m_R	m_R	1

	Zone-axis symmetries			
Point group	⟨111⟩	⟨100⟩	⟨*uv*0⟩	[*uvw*]
$m3$	6_R	$2mm1_R$	$2_R mm_R$	2_R
23	3	$2m_R m_R$	m_R	1

	Zone-axis symmetries						
Point group	[0001]	⟨11$\bar{2}$0⟩	⟨1$\bar{1}$00⟩	[*uv*.0]	[*uu*.*w*]	[*u*$\bar{u}$.*w*]	[*uv*.*w*]
$6/mmm$	$6mm1_R$	$2mm1_R$	$2mm1_R$	$2_R mm_R$	$2_R mm$	$2_R mm_R$	2_R
$\bar{6}m2$	$3m1_R$	$m1_R$	$2mm$	m	m_R	m	1
$6mm$	$6mm$	$m1_R$	$m1_R$	m_R	m	m	1
622	$6m_R m_R$	$2m_R m_R$	$2m_R m_R$	m_R	m_R	m_R	1

	Zone-axis symmetries		
Point group	[0001]	[*uv*.0]	[*uv*.*w*]
$6/m$	61_R	$2_R mm_R$	2_R
$\bar{6}$	31_R	m	1
6	6	m_R	1

	Zone-axis symmetries			
Point group	[0001]	⟨11$\bar{2}$0⟩	[*u*$\bar{u}$.*w*]	[*uv*.*w*]
$\bar{3}m$	$6_R mm_R$	21_R	$2_R mm_R$	2_R
$3m$	$3m$	1_R	m	1
32	$3m_R$	2	m_R	1

	Zone-axis symmetries	
Point group	[0001]	[*uv*.*w*]
$\bar{3}$	6_R	2_R
3	3	1

	Zone-axis symmetries						
Point group	[001]	⟨100⟩	⟨110⟩	[*u*0*w*]	[*uv*0]	[*uuw*]	[*uvw*]
$4/mmm$	$4mm1_R$	$2mm1_R$	$2mm1_R$	$2_R mm_R$	$2_R mm_R$	$2_R mm_R$	2_R
$\bar{4}2m$	$4_R mm_R$	$2m_R m_R$	$m1_R$	m_R	m_R	m	1
$4mm$	$4mm$	$m1_R$	$m1_R$	m	m_R	m	1
422	$4m_R m_R$	$2m_R m_R$	$2m_R m_R$	m_R	m_R	m_R	1

	Zone-axis symmetries		
Point group	[001]	[*uv*0]	[*uvw*]
$4/m$	41_R	$2_R mm_R$	2_R
$\bar{4}$	4_R	m_R	1
4	4	m_R	1

	Zone-axis symmetries				
Point group	[001]	⟨100⟩	[*u*0*w*]	[*uv*0]	[*uvw*]
mmm	$2mm1_R$	$2mm1_R$	$2_R mm_R$	$2_R mm_R$	2_R
$mm2$	$2mm$	$m1_R$	m	m_R	1
222	$2m_R m_R$	$2m_R m_R$	m_R	m_R	1

Table 2.5.3.4 (*cont.*)

Point group	Zone-axis symmetries		
	[010]	[*u*0*w*]	[*uvw*]
2/*m*	21_R	$2_R mm_R$	2_R
m	1_R	*m*	1
2	2	m_R	1

Point group	Zone-axis symmetry
	[*uvw*]
$\bar{1}$	2_R
1	1

the CBED symmetries for the two crystal (or incident-beam) settings which excite respectively the $+G$ and $-G$ reflections are drawn because the vertical rotation axes create the SMB patterns at different incident-beam orientations. [This had already been experienced for the case of symmetry 2_R (Goodman, 1975; Buxton *et al.*, 1976).] In the rectangular four-beam case, the symmetries for four settings which excite the $+G$, $+H$, $-G$ and $-H$ reflections are shown. For the diffraction groups $3m$, $3m_R$, $3m1_R$ and $6_R mm_R$, two different patterns are shown for the two crystal settings, which differ by $\pi/6$ rad from each other about the zone axis. Similarly, for the diffraction group $4_R mm_R$, two different patterns are shown for the two crystal settings, which differ by $\pi/4$ rad. Illustrations of these different symmetries are given in Fig. 2.5.3.7. The combination of the vertical threefold axis and a horizontal mirror plane introduces a new CBED symmetry 3_R. Similarly, the combination of the vertical sixfold rotation axis and an inversion centre introduces a new CBED symmetry 6_R.

There is an empirical and conventional technique for reproducing the symmetries of the SMB patterns which uses three operations of two-dimensional rotations, a vertical mirror at the centre of disc *O* and a rotation of π about the centre of a disc (1_R) without involving the reciprocal process. For example, we may consider 3_R between discs *F* and *F*′ in Table 2.5.3.5 in the case of diffraction group 31_R. Disc *F*′ is rotated anticlockwise not about the zone axis but *about the centre of disc O* by $2\pi/3$ rad (symbol 3) to coincide with disc *F*, and followed by a rotation of π rad (symbol *R*) about the centre of disc *F*′, resulting in the correct symmetry seen in Fig. 2.5.3.7. When the symmetries appearing between different SMB patterns are considered, this technique assumes that the symmetry operations are conducted after discs *O* and $\bar{O}$ are superposed. Another assumption is that the vertical mirror plane perpendicular to the line connecting discs *O* and $\bar{O}$ acts at the centre of disc *O* when the symmetries between two SMB patterns are considered. As an example, symmetry 3_R between discs *S* and $\bar{S}$ appearing in the two SMB patterns is reproduced by a threefold anticlockwise rotation of disc *S* about the centre of disc *O* (or $\bar{O}$) and followed by a rotation of π rad (*R*) about the centre of disc $\bar{S}$.

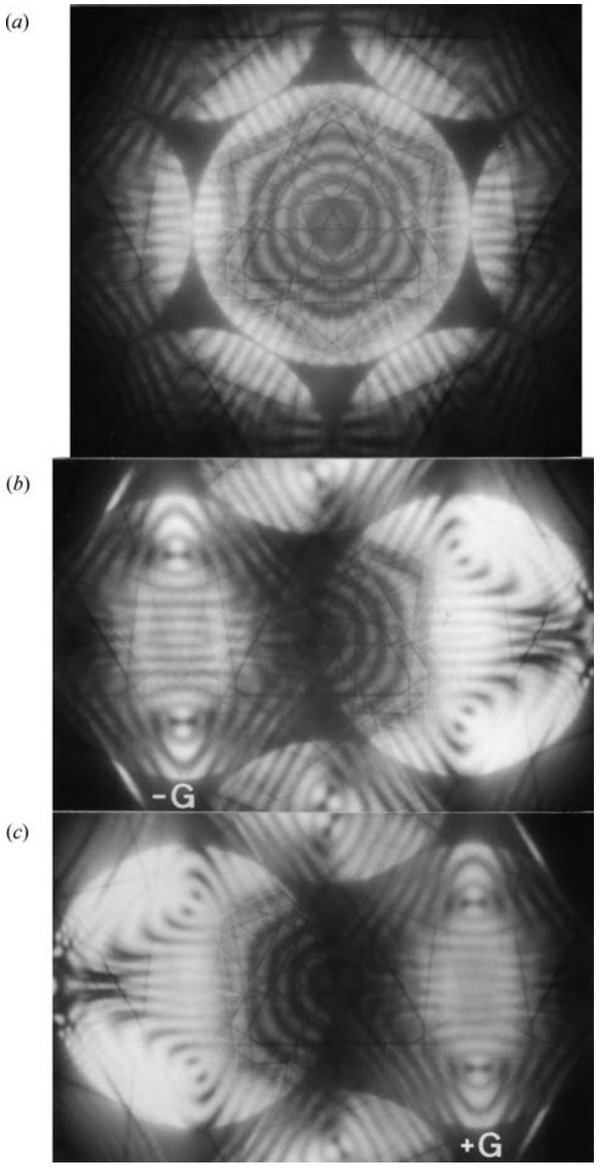

Fig. 2.5.3.5. CBED patterns of Si taken with the [111] incidence. (*a*) BP and WP show symmetry $3m_v$. (*b*) and (*c*) DPs show symmetry m_2 and DP symmetry $2_R m_{v'}$.

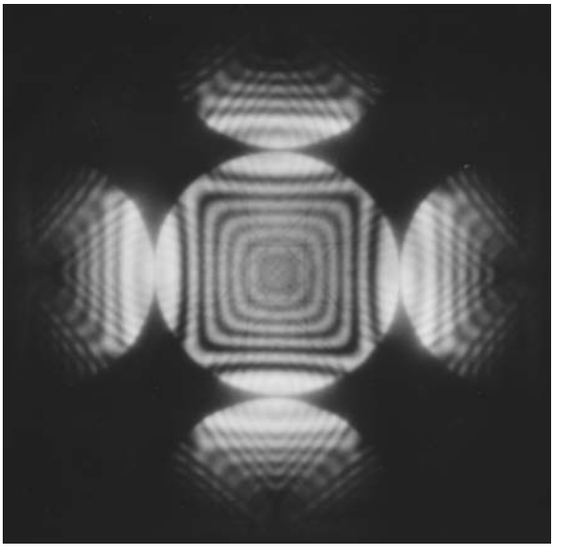

Fig. 2.5.3.6. CBED pattern of Si taken with the [100] incidence. The BP and WP show symmetry 4*mm*.

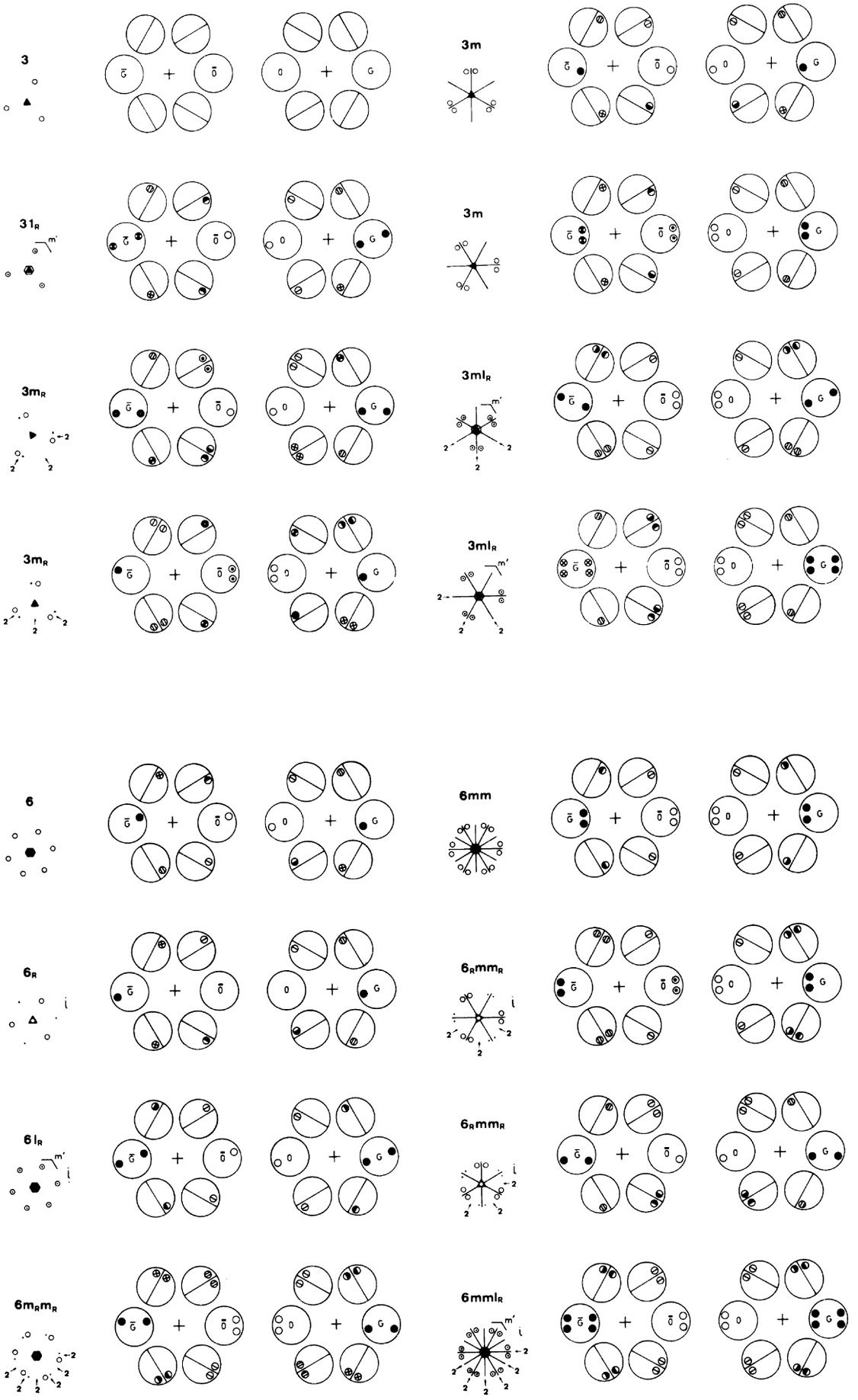

Fig. 2.5.3.7. Illustration of symmetries appearing in hexagonal six-beam, square four-beam and rectangular four-beam dark-field patterns expected for all the diffraction groups except for 1, 1_R, 2, 2_R and 21_R.

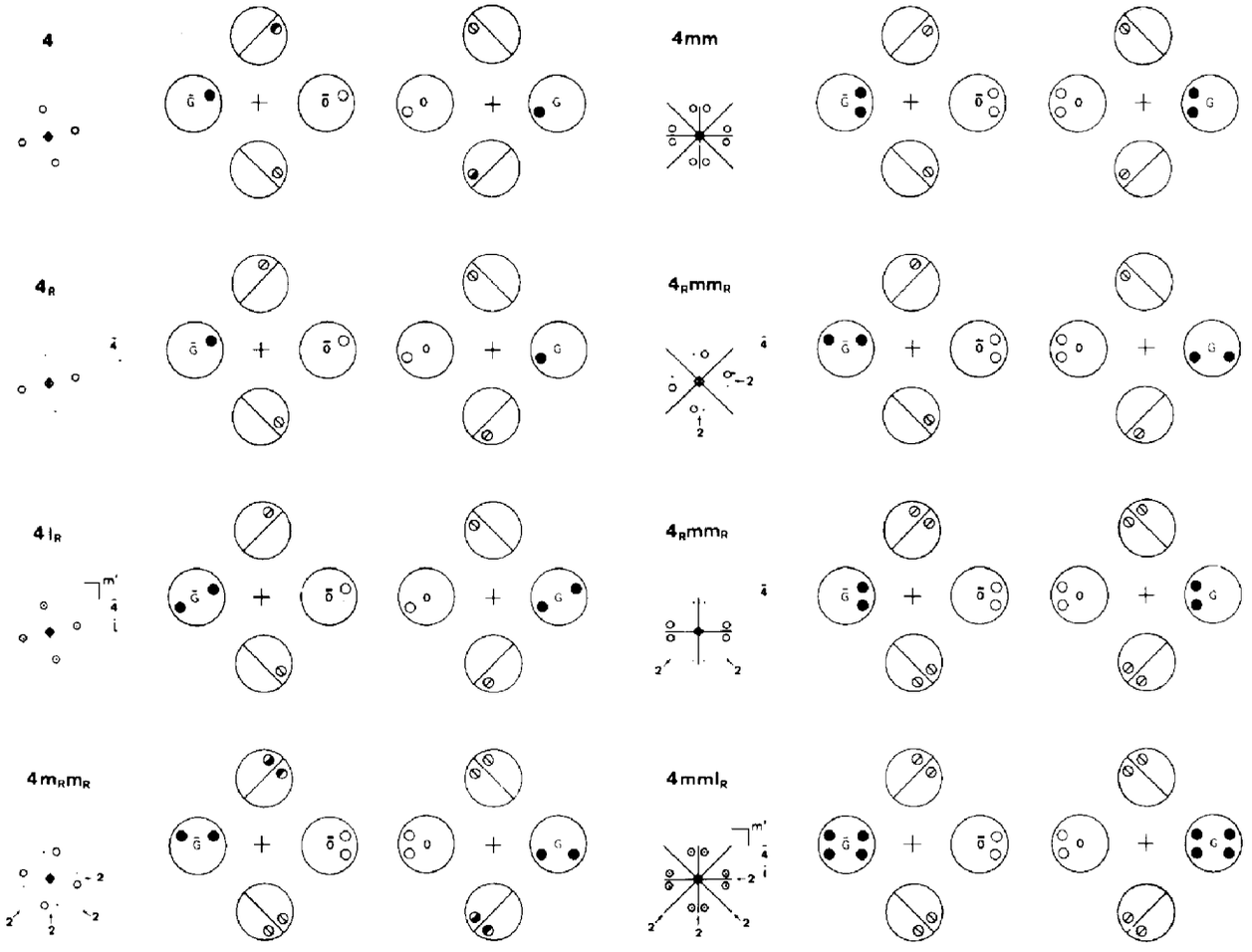

Fig. 2.5.3.7 (*cont.*).

Tables 2.5.3.5, 2.5.3.6 and 2.5.3.7 express the symmetries illustrated in Fig. 2.5.3.7 with the symmetry symbols for the hexagonal six-beam case, square four-beam case and rectangular four-beam case, respectively. In the fourth rows of the tables the symmetries of zone-axis patterns (BP and WP) are listed because combined use of the zone-axis pattern and the SMB pattern is efficient for symmetry determination. In the fifth row, the symmetries of the SMB pattern are listed. In the following rows, the symmetries appearing between the two SMB patterns are listed because the SMB symmetries appear not only in an SMB pattern but also in the pairs of SMB patterns. That is, for each diffraction group, all the possible SMB symmetries appearing in a pair of symmetric six-beam patterns, two pairs AB and AC of the square four-beam patterns and three pairs AB, AC and AD of the rectangular four-beam patterns are listed, though such pairs are not always needed for the determination of the diffraction groups. It is noted that the symmetries in parentheses are the symmetries which add no new symmetries, even if they are present. In the last row, the point groups which cause the diffraction groups listed in the first row are given.

By referring to Tables 2.5.3.5, 2.5.3.6 and 2.5.3.7, the characteristic features of the SMB method are seen to be as follows. CBED symmetry m_2 due to a horizontal twofold rotation axis can appear in every disc of an SMB pattern. Symmetry 1_R due to a horizontal mirror plane, however, appears only in disc G or H of an SMB pattern. In the hexagonal six-beam case, an inversion centre i produces CBED symmetry 6_R between discs S and S' due to the combination of an inversion centre and a vertical threefold rotation axis (and/or of a horizontal mirror plane and a vertical sixfold rotation axis). This indicates that one hexagonal six-beam pattern can reveal whether a specimen has an inversion centre or not, while the method of Buxton *et al.* (1976) requires two photographs for the inversion test. All the diffraction groups in Table 2.5.3.5 can be identified from one six-beam pattern except groups 3 and 6. Diffraction groups 3 and 6 cannot be distinguished from the hexagonal six-beam pattern because it is insensitive to the vertical axis. In the square four-beam case, fourfold rotary inversion $\bar{4}$ produces CBED symmetry 4_R between discs F and F' in one SMB pattern, while Buxton *et al.*'s method requires four photographs to identify fourfold rotary inversion. Although an inversion centre itself does not exhibit any symmetry in the square four-beam pattern, it causes symmetry 1_R due to the horizontal mirror plane produced by the combination of an inversion centre and the twofold rotation axis. Thus, symmetry 1_R is an indication of the existence of an inversion centre in the square four-beam case. All of the seven diffraction groups in Table 2.5.3.6 can be identified from one square four-beam pattern. One rectangular four-beam pattern can distinguish all the diffraction groups in Table 2.5.3.7 except the groups m and $2mm$. It is emphasized again that the inversion test can be carried out using one six-beam pattern or one square four-beam pattern.

Fig. 2.5.3.8 shows CBED patterns taken from a [111] pyrite (FeS_2) plate with an accelerating voltage of 100 kV. The space group of FeS_2 is $P2_1/a\bar{3}$. The diffraction group of the plate is 6_R due to a threefold rotation axis and an inversion centre. The zone-axis pattern of Fig. 2.5.3.8(a) shows threefold rotation symmetry in the BP and WP. The hexagonal six-beam pattern of Fig. 2.5.3.8(b) shows no symmetry higher than 1 in discs O, G, F and S but shows symmetry 6_R between discs S and S', which

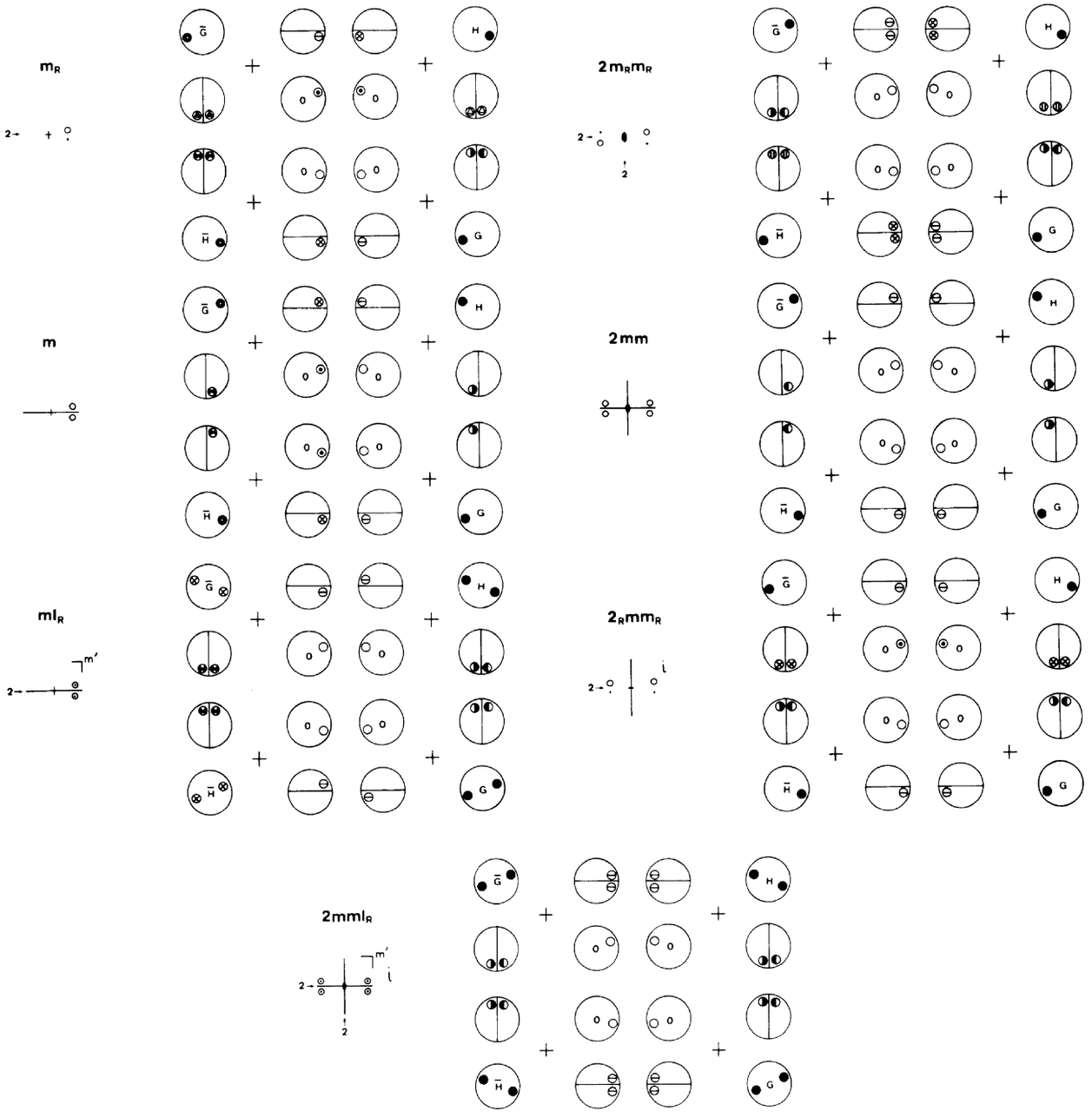

Fig. 2.5.3.7 (*cont.*).

proves the existence of a threefold rotation axis and an inversion centre. The same symmetries are also seen in Fig. 2.5.3.8(*c*), where reflections $\bar{O}$, $\bar{G}$, $\bar{F}$, $\bar{S}$, $\bar{F}'$ and $\bar{S}'$ are excited. Table 2.5.3.5 indicates that diffraction group 6_R can be identified from only one hexagonal six-beam pattern, because no other diffraction groups give rise to the same symmetries in the six discs. When Buxton *et al.*'s method is used, three photographs or four patterns are necessary to identify diffraction group 6_R (see Table 2.5.3.3). In addition, if the symmetries between Figs. 2.5.3.8(*b*) and (*c*) are examined, symmetry 2_R between discs G and $\bar{G}$ and symmetry 6_R between discs F and $\bar{F}$ are found. All the experimental results agree exactly with the theoretical results given in Fig. 2.5.3.7 and Table 2.5.3.5.

Fig. 2.5.3.9 shows CBED patterns taken from a [110] V_3Si plate with an accelerating voltage of 80 kV. The space group of V_3Si is $Pm3n$. The diffraction group of the plate is $2mm1_R$ due to two vertical mirror planes and a horizontal mirror plane, a twofold rotation axis being produced at the intersection line of two perpendicular mirror planes. The zone-axis pattern of Fig. 2.5.3.9(*a*) shows symmetry $2mm$ in the BP and WP. The rectangular four-beam pattern of Fig. 2.5.3.9(*b*) shows symmetry 1_R in disc H due to the horizontal mirror plane and symmetry m_2 in both discs $\bar{S}$ and F' due to the twofold rotation axes in the [001] and [110] directions, respectively. The same symmetries are also seen in Fig. 2.5.3.9(*c*), where reflections $\bar{H}$, S' and $\bar{F}$ are excited. Table 2.5.3.7 implies that the diffraction group $2mm1_R$ can be identified from only one rectangular four-beam pattern, because no other diffraction groups give rise to the same symmetries in the four discs. When Buxton *et al.*'s method is used, two photographs or three patterns are necessary to identify diffraction group $2mm1_R$ (see Table 2.5.3.3). One can confirm the theoretically predicted symmetries between Fig. 2.5.3.9(*b*) and Fig. 2.5.3.9(*c*). All the experimental results agree exactly with the theoretical results given in Fig. 2.5.3.7 and Table 2.5.3.7.

These experiments show that the SMB method is quite effective for determining the diffraction group of slabs. Buxton *et al.*'s method identifies two-dimensional symmetry elements in the first place using a zone-axis pattern, and three-dimensional symmetry elements using DPs. On the other hand, the SMB method primarily finds many three-dimensional symmetry elements in an

Table 2.5.3.5. *Symmetries of hexagonal six-beam CBED patterns for diffraction groups*

		Projection diffraction group									
		31_R		$3m1_R$					61_R		
Diffraction group		3	31_R	$3m_R$		$3m$		$3m1_R$	6	6_R	61_R
Two-dimensional symmetry		3	3	3		$3m$		$3m$	6	3	6
Three-dimensional symmetry			m'	$2'$				m', $(2')$		i	m', (i)
Zone-axis pattern	Bright-field pattern	3	6	$3m$		$3m$		$6mm$	6	3	6
	Whole-field pattern	3	3	3		$3m$		$3m$	6	3	6
Hexagonal six-beam pattern	O	1	1	1	m_2	1	m_v	m_2	m_v	1	1	1
	G	1	1_R	m_2	1	1	m_v	1_R	$1_R m_v(m_2)$	1	1	1_R
	F	1	1	m_2	1	1	1	1	m_2	1	1	1
	S	1	1	1	m_2	1	1	m_2	1	1	1	1
	FF'	1	3_R	1	1	1	m_v	3_R	$3_R m_v$	1	1	3_R
	SS'	1	1	1	1	1	m_v	1	m_v	1	6_R	6_R
A pair of symmetrical six-beam patterns 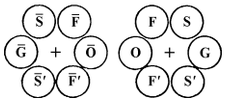	$\pm O$	1	1_R	m_2	1	m_v	1	$m_v 1_R$	$1_R m_2$	2	1	$2(1_R)$
	$\pm G$	1	1	1	m_R	m_v	1	$m_v m_R$	1	2	2_R	21_R
	$\pm F$	1	1	1	1	m_v	1	m_v	1	1	6_R	6_R
	$\pm S$	1	3_R	1	1	m_v	1	$3_R m_v$	3_R	1	1	3_R
	$F'\bar{F}$	1	1	1	m_R	1	1	m_R	1	2	1	2
	$S'\bar{S}$	1	1	m_R	1	1	1	1	m_R	2	1	2
Point group		23, 3	$\bar{6}$	432, 32		$\bar{4}3m$, $3m$		$\bar{6}m2$	6	$m3$, 3	$6/m$

		Projection diffraction group				
		$6mm1_R$				
Diffraction group		$6m_R m_R$	$6mm$	$6_R mm_R$		$6mm1_R$
Two-dimensional symmetry		6	$6mm$	$3m$		$6mm$
Three-dimensional symmetry		$2'$		i, $(2')$		m', $(i, 2')$
Zone-axis pattern	Bright-field pattern	$6mm$	$6mm$	$3m$		$6mm$
	Whole-field pattern	6	$6mm$	$3m$		$6mm$
Hexagonal six-beam pattern	O	m_2	m_v	1	$m_v(m_2)$	$m_v(m_2)$
	G	m_2	m_v	m_2	m_v	$1_R m_v(m_2)$
	F	m_2	1	m_2	1	m_2
	S	m_2	1	1	m_2	m_2
	FF'	1	m_v	1	m_v	$3_R m_v$
	SS'	1	m_v	6_R	$6_R m_v$	$6_R m_v$
A pair of symmetrical six-beam patterns 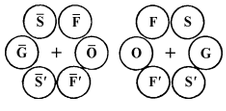	$\pm O$	$2m_2$	$2m_{v'}$	$m_v(m_2)$	1	$2(1_R)m_{v'}(m_2)$
	$\pm G$	$2m_R$	$2m_{v'}$	$2_R m_v$	$2_R m_R$	$21_R m_{v'}(m_R)$
	$\pm F$	1	$m_{v'}$	$6_R m_v$	6_R	$6_R m_{v'}$
	$\pm S$	1	$m_{v'}$	m_v	1	$3_R m_{v'}$
	$F'\bar{F}$	$2m_R$	2	1	m_R	$2m_R$
	$S'\bar{S}$	$2m_R$	2	m_R	1	$2m_R$
Point group		622	$6mm$	$m3m$, $\bar{3}m$		$6/mmm$

SMB pattern, and two-dimensional symmetry elements from a pair of SMB patterns, as shown in Tables 2.5.3.5, 2.5.3.6 and 2.5.3.7. Therefore, the use of a ZAP and SMB patterns is the most efficient way to find as many crystal symmetry elements in a specimen as possible.

2.5.3.3. Space-group determination

2.5.3.3.1. Lattice-type determination

When the point group of a specimen crystal is determined, the crystal axes may be found from a spot diffraction pattern recorded at a high-symmetry zone axis, using the orientations of the symmetry elements determined in the course of point-group determination. Integral-number indices are assigned to the spots of the diffraction patterns. The systematic absence of reflections indicates the lattice type of the crystal. It should be noted that reflections forbidden by the lattice type are always absent, even if dynamical diffraction takes place. (This is true for all sample thicknesses and accelerating voltages.) By comparing the experimentally obtained absences and the extinction rules known for the lattice types [P, C (A, B), I, F and R], a lattice type may be identified for the crystal concerned.

2.5.3.3.2. Identification of screw axes and glide planes

There are three space-group symmetry elements of diperiodic plane figures: (1) a horizontal screw axis $2'_1$, (2) a vertical glide plane g with a horizontal glide vector and (3) a horizontal glide plane g'. These are related to the point-group symmetry elements $2'$, m and m' of diperiodic plane figures, respectively. (It is noted that these symmetry elements and ten point-group symmetry elements form 80 space groups.)

references